Accepted Manuscript

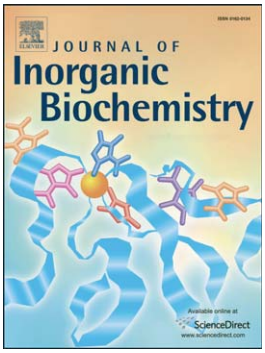

Synthesis, characterisation and biological activities of semicarbazones and their copper complexes

Taracad K. Venkatachalam, Paul V. Bernhardt, Chris J. Noble, Nicholas Fletcher, Gregory K. Pierens, Kris J. Thurecht, David C. Reutens

PII: S0162-0134(16)30093-9
DOI: doi: 10.1016/j.jinorgbio.2016.04.006
Reference: JIB 9964

To appear in: *Journal of Inorganic Biochemistry*

Received date: 23 November 2015
Revised date: 21 March 2016
Accepted date: 3 April 2016

Please cite this article as: Taracad K. Venkatachalam, Paul V. Bernhardt, Chris J. Noble, Nicholas Fletcher, Gregory K. Pierens, Kris J. Thurecht, David C. Reutens, Synthesis, characterisation and biological activities of semicarbazones and their copper complexes, *Journal of Inorganic Biochemistry* (2016), doi: 10.1016/j.jinorgbio.2016.04.006

Synthesis, characterisation and biological activities of semicarbazones and their copper complexes.

Taracad K. Venkatachalam*, Paul V. Bernhardt[#], Chris J. Noble, Nicholas Fletcher, Gregory K. Pierens, Kris J. Thurecht, David C. Reutens*

Centre for Advanced Imaging, [#]School of Chemistry University of Queensland, St.Lucia, Brisbane 4072, Australia. -

* Corresponding author: t.venkatachalam@uq.edu.au

Keywords: Synthesis, Characterization, Semicarbazones, Copper complex, X-ray crystallography - Biological activity,

Abstract: Substituted semicarbazones/thiosemicarbazones and their copper complexes have been prepared and several single crystal structures examined. The copper complexes of these semicarbazone/thiosemicarbazones were prepared and several crystal structures examined. The single crystal X-ray structure of the pyridyl-substituted semicarbazone showed two types of copper complexes, a monomer and a dimer. We also found that the p-nitrophenyl semicarbazone formed a conventional 'magic lantern' acetate-bridged dimer. Electron Paramagnetic Resonance (EPR) of several of the copper complexes were *c*onsistent with the results of single crystal X-ray crystallography. The EPR spectra of the p-nitrophenyl semicarbazone copper complex in dimethylsulfoxide (DMSO) showed the presence of two species, confirming the structural information. Since thiosemicarbazones and semicarbazones have been reported to exhibit anticancer activity, we examined the anticancer activity of several of the derivatives reported in the present study and interestingly only the thiosemicarbazone showed activity while the semicarbazones were not active indicating that introduction of sulphur atom alters the biological profile of these thiosemicarbazones.

This paper is dedicated in memory of Prof. Graeme Hanson, a friend, scholar and mentor for his dedicated and tireless contribution to science.

Introduction:

Thiosemicarbazones and semicarbazones are important classes of compounds that coordinate with many metal ions because of the presence of several donor atoms such as nitrogen, oxygen and sulphur in their structural core. The preparation and characterization of diversely substituted thiosemicarbazones/semicarbazones have been explored as early as the 1950s[1] and coordination of these compounds with metal ions were extensively studied in the 1960s[2] Although these early discoveries were milestones in the development of thiosemicarbazone/semicarbazone compounds, the lack of structural evidence, for example X-ray single crystal structure, may raise doubts about the architecture of some of the metal complexes. Lobana et.al [3] have compiled a detailed review on the bonding and structural characteristics of thiosemicarbazones in particular, and reported the development of newer strategies for preparing newer derivatives. In the recent years attention has focussed on the biological applications of these compounds. In this regard, it has been found that some thiosemicarbazones have potent anticancer activity [4-14] The use of iron chelators containing thiosemicarbazones has also been extensively studied [15-26] as has the anticancer activity of novel thiosemicarbazones generated through the combination of retro fragments. Some thiosemicarbazones have been found to have antibacterial and antifungal activity [27-29] and the pharmacological profile of thiosemicarbazones attached to a heterocyclic core has been reported by Singhal et al [30] The biological profile exhibited by these thiosemicarbazone and semicarbazone derivatives has led to work in which these compounds have been complexed with positron emitting isotopes (e.g. ^{64}Cu, ^{68}Ga) for use as imaging agents. The radio-metal complexes (most notably ^{64}Cu) of these ligands have been investigated for their applications as molecular imaging agents. [31-37] Pascu et al [38-40] have synthesized a series of ^{68}Ga complexes of bis-thiosemicarbazones to evaluate their imaging potential. Interestingly, they report that the reaction of $GaCl_3$ with these ligands results in the formation of a square based pyramidal mono-chloride metal complex, prompting us to propose the potential of exchanging this chloride with other ligands, particularly other halogens. This paper describes the copper complexes of semicarbazones which are relevant to PET (Positron emission tomography)

imaging however the corresponding iron or manganese complexes can be utilized as contrast agents for magnetic resonance imaging. We were specifically interested in the recent application of coordination complexes of Group 13 metal ions with fluoride. McBride et al and others [41-48] have reported the formation of inorganic aluminium complexes with the radioisotope ^{18}F which show excellent stability, and have highlighted that these provide simple moieties which can be incorporated into a wide range of biomolecules with potential as positron emitting tomography (PET) imaging agents. We prepared new semicarbazones and thiosemicarbazones and their copper complexes, studied their structural characteristics and evaluated their biological profiles.

Experimental: All chemicals were obtained from Sigma Aldrich and were used without further purification. NMR spectra (Nuclear Magnetic Resonance) were recorded in d_6-DMSO) (deuterated DMSO) and the chemical shifts are reported relative to DMSO at 2.54 ppm. The NMR data were acquired on a Bruker 700 MHz NMR spectrometer equipped with a cryoprobe. The proton spectra where acquired with a sweep width of 18 ppm cantered at 7 ppm. The carbon spectra were acquired with a sweep width of 220 ppm centered at 110 ppm. The COSY (Correlation Spectroscopy) experiments were acquired with a sweep width of 18 ppm using a 90° pulse of 9 µs with 256 increments respectively. The ^{13}C HSQC spectra (Heteronuclear Single Quantum Correlation) were acquired with sweep widths of 18 and 160 ppm for proton and carbon respectively and the carbon centered at 80 ppm. Additionally HMBC (Heteronuclear Multiple Bond Correlation*)* spectral data were also acquired to establish the structures of the compounds (^{13}C sweep width of 220 ppm). The raw data were usually multiplied by an exponential or shifted sine squared function before performing the Fourier transform. DOSY spectra (Diffusion-ordered spectroscopy) were done using standard parameters. UV/Visible spectra (Ultraviolet/Visible) were obtained using a Thermoscientific Nanodrop model 2000C Spectrophotometer using methanol or DMSO as solvent. The IR (Infrared) spectra were acquired using a Nicolet Diamond model 5700 Fourier Transform Infrared spectrometer. The samples were used as powders and introduced in the spectrometer. For other samples, chloroform was used as a solvent and was allowed to evaporate before obtaining IR spectra.

Molecular Modeling: Monte Carlo Conformational (MCMM) searching was performed using Macromodel v10.0 (Schrodinger, New York) for syn and anti-isomers. Torsional sampling (MCMM) performed with 1000 steps per rotatable bond. Each step was minimised with the OPLS-2005 (polarizable and non polarizable) force field using the TNCG (Truncated Newton Conjugate Gradient) method with maximum iterations of 50,000 and energy convergence threshold of 0.02. All other parameters were left as the default values. The lowest energy conformations (< 3 kcal/mol from global minimum, were further optimised using DFT (Density Functional Theory) calculations in Gaussian (B3LYP/6311+G (d,p), with DMSO solvent).

Synthesis of semicarbazones and thiosemicarbazones: The appropriate aldehyde (0.05 mol) thiosemicarbazone (0.025 mol), anhydrous sodium acetate (2.0g), ethanol (20 ml) and water (20ml) were stirred for 10 minutes. After this period, concentrated hydrochloric acid (0.5 ml) was added and the mixture was stirred overnight when a clear solution resulted. The precipitate was filtered and washed with ethanol and dried under vacuum. Further purification was achieved by recrystallization from methanol. The characterization data of the individual ligands used in the present study have been disclosed in our earlier publication[49].(see supporting information)

Copper complex formation: To a stirred solution of the thiosemicarbazones/thiosemicarbazones in methanol (1 mmol or 2 mmol) was added the appropriate copper salt (0.5 mmol or 1 mmol).The contents were allowed to reflux for 3 hours when a precipitate started appearing. The solution was cooled and the solid was filtered, washed with methanol and ether and subsequently dried in vacuum to furnish complexes with varying colors from green to orange red.

Characterization data of selected copper complexes of ligands:

L1: UV (MeOH) 250-350 (multiple peaks), 699nm. IR: 3469, 3220, 1699, 1646, 1576, 1569, 1472, 1466, 1436, 1420, 1342, 1093, 851, 758, 688, 515, 461 cm^{-1}.

L3: UV (acetone): 253, 372 nm; IR: 3306, 3282, 3102, 1637, 1604, 1559, 1466, 1445, 1408, 1369, 1317, 1230, 1167, 1154, 1106, 1016, 917, 883, 738, 546, 451, 438 cm^{-1}.

L4: UV (acetone):326,370 and 690 nm; IR: 3411, 3194, 1691, 1569, 1498, 1396, 1240, 1150, 1086, 1023, 826, 683, 561, 533, 451 cm^{-1}

L5: UV (not soluble), IR: 3306, 3282, 3101, 1636, 1604, 1558, 1465, 1445, 1418, 1316, 1301, 1230, 1157, 1105, 917, 737, 672, 624, 547, 451, 439 cm^{-1}.

L6-: UV ($MeOH/CH_2Cl_2$):252, 350, 680nm; IR: 3301, 3199, 3034, 1639, 1605, 1580, 1557, 1519, 1417, 1347, 1339, 1227, 1101, 1095, 776, 648, 519, 446 cm^{-1}.

EPR measurements details:

X-band CW-EPR (Continuous Wave Electron Paramagnetic Resonance) power saturation measurements: CW-EPR spectra were measured with a Bruker Biospin Elexsys E500 CW-EPR spectrometer. The spectrometer had a 10in electromagnet in conjuction with a 12kW power supply (fields upto 1.4T), X-band (9-10GHz), a microwave bridge and a high Q cavity. This high Q cavity or quality factor indicates how efficiently the cavity stores microwave energy. As Q increases, the sensitivity of the spectrometer increases and this factor is defined by the ratio between the energy stored and energy dissipated per cycle. It also possesed a 4131VT variable temperature unit connected by a liquid nitrogen gas flow tube.This was purposely used to ensure that the temperature of the sample is kept constant throughout the EPR measurements. Additionally the spectrometer consists of a Brucker Biospin teslameter (ER036TM) and an eIP 548B fequency counter.These counters were able to monitor the magnetic field calibrations as well as the microwave frequency. A integrated PC system with Mandriva Linux and the Bruker Biospin Xepr (v 2.66.45) was used to acquire data and to control the spectrometer. The Xepr (X-band Electron Paramagnetic Resonance) was used to measure multidimensional EPR data sets during an experiment.

Sample Preparation: The copper complexes of the semicarbazones and thiosemicarbazones were prepared by dissoling a known quantity (approximately 5mg) of the compounds in either methanol or dimethyl sulfoxide (3 ml). The homogenous solution was carefully transferred into the EPR tube by pasteur pipette so that the sample volume remained well below $1/5^{th}$ of the EPR tube length (approximately 3cm). The sample was then frozen using liquid nitrogen in a dewar and the frozen

sample was quickly transferred into the precooled cavity of the EPR spectrometer. For 2-pyridylthiosemicarbazonecopper the spectrum was recorded at microwave frequency = 9.3710 GHz, microwave power = 2mW, modulation amplitude =1G, temperature=140K, For 2-nitrophenylthiosemicarbazonecopper the spectrum was recorded at microwave frequency = 9.4331 GHz, microwave power = 20mW, modulation amplitude = 4G, temperature = 140K, EPR spectrum of 4-nitrophenylsemicarbazonecopper(**C3&C2**) a) recorded at microwave frequency = 9.4348 GHz, microwave power = 20mW, modulation amplitude =4G, temperature = 140K, (see discussion on monomer and dimer formation in X-ray crystallography**).**

Biological assay:

PC-3 human prostate cancer cell line was purchased from the American Type Culture Collection (ATCC) and maintained in RPMI-1640 medium (Rosewell Park Memorial Institute) (Gibco, Thermo Fisher Scientific) supplemented with 10% (v/v) Foetal Bovine Serum (FBS; Bovogen, Australia), 50 $U.ml^{-1}$ penicillin, 50 $\mu g.ml^{-1}$ streptomycin and 2 mM L-glutamine (Gibco, Thermo Fisher Scientific). Cells were grown in a 37 °C incubator with 5% CO_2/air and passaged every 3-4 days.

For cytotoxicity assays, 2 mg of each compound was dissolved in DMSO (Sigma Aldrich, hybri-max grade) to give a final concentration of 10 mg/mL for the ligands alone and 5 mg/mL for the ligands with copper. DMSO stock solutions were diluted into cell culture media with rapid mixing to give a final concentration of 100 µM test compound. The test compound solutions were prepared by dilution of dimethyl sulfoxide (DMSO) stocks of synthesized compounds into cell culture media which was then sterile filtered (0.22 µm; Millex, Millipore). and serially diluted to give media with 50 and 10 µM of the compound. Final DMSO concentrations in media were 0.5 % (v/v) and 1.3 % (v/v) for ligands alone and ligands with copper respectively Final DMSO concentrations in media were <1.3% (v/v) and cellular proliferation was compared to control wells containing equivalent concentrations of DMSO with no test compound. Cells were seeded at 5,000 cells per well of 96-well plates and allowed to adhere in growth media overnight. Cells were then incubated with fresh growth media (100 µL) containing synthesized chelators ± copper at 10, 50 or 100 µM (each in triplicate) for approximately 48 hours in a 37 °C incubator with 5% CO_2/air. Cell viability was then assessed by 3-

(4,5-dimethylthiazol-2-yl)-5-(3-carboxymethoxyphenyl)-2-(4-sulfophenyl)-2H-tetrazolium (MTS) assay (CellTiter 96 AQuesous One Solution Cell Proliferation Assay; Promega) following provided manufacturers methods. Briefly, wells were washed once with 200 µL growth media before addition of 100 µL of growth media containing 20% (v/v) MTS assay reagent. Plates were incubated for 1-2 hours at 37 °C and absorbance at 490 nm of each well was measured. Absorbance readings of blank wells (no cells) were subtracted from all readings and then values were normalized (taking into account the values for DMSO alone) to cells grown in the absence of test compounds. Where necessary IC_{50} values for tested compounds were estimated using fitting of data using the Graphpad Prism Software version 6.05 (Graphpad Software).

X-ray crystallography: **X-ray crystallography**: X-ray quality single crystals were obtained by slow diffusion of methanol to dichloromethane solution. Crystallographic data were acquired at 190 K on an Oxford Diffraction Gemini CCD diffractometer employing either Mo Kα radiation (0.71073 Å) or Cu Kα radiation (1.5418 Å) and operating in the ω-scan mode. Temperature control was achieved with an Oxford Cryosystems Desktop Cooler. Data reduction and empirical absorption corrections (multiscan) were performed with Oxford Diffraction CrysAlisPro software. The structure was solved by direct methods with SHELXS and refined by full-matrix least-squares analysis with SHELXL-97 [50] within the WinGX graphical user interface [51]. All non-H atoms were refined with anisotropic thermal parameters. The molecular structure diagrams were produced with ORTEP3 [52] or PLATON.[53] The data in CIF format have been deposited at the Cambridge Crystallographic Data Centre. The structure of C3 was determined with a non-merohedrally twinned specimen (partially overlapping reflections) and refinement was performed on both twin components (HKLF 5 function). The following CCDC numbers contains the complete X-ray crystallographic data and the data can be obtained free of charge via http://www.ccdc.cam.ac.UK/conts/retreiving or from the Cambridge crystallography data centre. CCDC numbers: 1436285 – 1436289.

Results and Discussion: Thiosemicarbazones and semicarbazones were synthesized following Schemes 1 and 2 shown below. In brief, appropriate aldehydes were treated with thiosemicarbazide or

semicarbazide in ethanol medium in the presence of sodium acetate to furnish the required thiosemicarbazones in good yield. The crude samples were further purified by re-crystallization using ethanol. The characterization data of individual semicarbazones and thiosemicarbazones have been disclosed in an earlier publication from this laboratory [49] The UV spectra of all the thiosemicarbazones in chloroform showed peaks at 309-330nm corresponding to the pi-pi transitions.(See supporting information) However the UV spectra of individual copper complexes had distinct peaks at various wavelengths. For example the 2-pyridyl semicarbazone had a visible peak at 660nm followed by a strong absorption peak at 355 nm in methanol/dchloromethane solvent. The 4- pyridyl thiosemicarbazone showed a similar trend and showed a strong absorption at 370nm. The p-nitro phenyl substituted semicarbazone showed a visible peak at 699nm followed by strong absorption peaks at 350 nm. The other thiosemicarbazones/semicarbazones showed similar trends in their UV/Visible spectral characteristics.

The IR spectra of the complexes were analysed and the p-nitrophenyl semicarbazone copper complex showed strong absorption at 1698-1647 cm^{-1} indicating the presence of a C=O group in the molecule. Several other stretching vibration bands were observed between 1341-1559cm^{-1} indicative of the aromatic nucleus and the C=N character. Additional stretching bands between 447-499 cm^{-1} showed the presence of a copper coordinated complex in the structure of the molecule. The 2-pyridyl substituted semicarbazone copper complex showed stretching vibration for the NH group between 3400-3200 cm^{-1} followed by a strong stretching band at 1605 cm^{-1} (C=O) and other stretching vibrations related to aromatic ring as well as C=N (1095-1518cm^{-1}). The presence of the copper coordination is further manifested by vibrational bands between 460-518 cm^{-1}. All the other thiosemicarbazones and semicarbazones exhibited a similar trend, confirming the presence of appropriate groups in the structure of the individual molecules. We also analysed infrared spectra of two additional new thiosemicarbazones with a furan and naphthyl ring in the structure in addition to the phenyl ring (Scheme 3).

The furan substituted thiosemicarbazone showed vibrational stretch between 3455-3294 cm^{-1} indicative of the NH stretching followed by a strong absorption band at 1625-1590 cm^{-1} (C=O) and the phenyl stretching vibrations including the C=N stretch (1356-1543 cm^{-1})

The NMR spectra of all the thiosemicarbazones and semicarbazones have been reported earlier [49] (see supporting information) and the NMR (^{1}H, ^{13}C, ^{15}N) chemical shift values demonstrate the appropriate groups attached to the structures of individual compounds.

Syn and anti-isomerism: Semicarbazones, thiosemicarbazones, phenyl hydrazones and oximes have the unique capability of forming syn and anti- isomers. Generally a mixture of isomers is synthesised depending on the experimental conditions used to prepare the compounds. An example of syn- and anti-isomers of a thiosemicarbazone is shown in Scheme 4.

It is evident from Scheme 4 that for the anti-isomer (E), the chemical environment of the NH proton should be different to syn (Z) isomer. This is due to the proton of the NH group being in closer proximity to the aromatic protons for the syn- isomer than the anti-isomer [54]. The NMR spectra for all the compounds reported in our study showed only one set of peaks, demonstrating the preferential formation of one isomer over the other or a fast exchange between the two isomers

To examine whether it is viable to synthesise any of the compounds in the present study as the syn isomer, the anti-isomers were refluxed in methanol using silica gel as a catalyst [54] Thin layer chromatography revealed that only 2-pyridyl thiosemicarbazone formed the syn isomer. A fresh sample of the syn isomer of 2-pyridyl thiosemicarbazone was prepared and dissolved in DMSO-d_6 and the proton NMR acquired. (see supporting information).

The NMR spectrum showed a peak at 14 ppm, similar to that reported by previous workers. [54-55] It was evident from the NMR that the chemical shift for the NH group protons as well as the aromatic protons associated with the structure of the molecule differs between isomers. The downfield shift of the NH protons for the syn thiosemicarbazone demonstrates that there is hydrogen bonding between the NH groups and the aromatic nitrogen. The ^{1}H spectrum was acquired at various time intervals over an 18 hour period. The peak at 14 ppm (H3, syn) decreased in intensity with a corresponding

increase in the peak at 11.6 ppm (H3, anti). A plot of the formation of the anti-isomer in Figure F1(see supporting information) follows a first order rate equation with a rate constant of $2.4x10^{-3}$/min. Figure F2 compares the starting ^{1}H NMR spectrum, the corresponding spectra approximately half way through the conversion and the final spectrum of the anti- compound and Figure F3 shows a ^{13}C HSQC at approximately 50% conversion showing the two isomers. In the case of copper complex of ligand 4, two types of crystals were obtained, and each of these crystals were dissolved in d_6-DMSO and the ^{1}H NMR spectra taken (see supporting document). As can be seen from the proton NMR spectra, the two crystals showed slight difference in chemical shift values of the aromatic protons associated with the structure of the ligand. The largest being from 9.32 to 8.68 ppm. Subsequently, a DOSY experiment was performed for the individual crystals and as can be seen from the over lay of individual DOSY spectra (see supporting document), both compounds showed a very similar diffusion coefficient.

Additionally, molecular modelling studies were undertaken. The compounds were initially investigated by a Monte Carlo conformational search (MacroModel, Schrodinger) and the conformations with 3 kcal/mol were then further optimized using DFT calculation (Gaussian 09) with the inclusion of the polarizable continuum model (IEF-PCM) and solvent model for DMSO and the 2-pyrdiyl thiosemicarbazone and the syn and anti-isomers had two different conformations with the lowest energy syn isomer (planar conformation) being 0.2 kcal/mol lower energy compared to the lowest anti isomer (planar conformation). The alternate conformation was much higher in energy. In the present study, the observed chemical shifts for this proton showed the preferential formation of anti-isomer due to its lower energy state. Both isomers were examined by DFT which showed that the anti- isomer was about 5.3 kcal/mol lower energy than the syn isomer explaining why only the anti-isomer was formed. The syn isomer was not planar due to steric interactions from the protons H7 and H11. (see supporting information)

Keto- enol tautomerism :

An interesting feature regarding the structure of semicarbazones is that in solid state most of the semicarbazones exhibit a keto form whereas in solution state they may exhibit keto-enol tautomerism as shown below in chart 1:

The keto form acts as a bidendate ligand while the enol form can lose the proton and act as an anionic bidendate ligand in complexes. Substituents on the aromatic ring can further enhance the electron density through delocalization enabling the semicarbazone to form chelate complexes with metal ions.

In the present study, the X-ray crystal solid state structure confirms that the semicarbazones exist in keto form as expected. The ^{13}C NMR spectrum of these compounds in solution state tend to show the same evidence for an keto form as evidenced from the chemical shift values of the carbon atom associated with the carbonyl oxygen of the semicarbazone.

X-ray crystal studies

The single crystal X-ray studies were conducted and the details are shown in the supporting documents for further reference**.** The crystal structure of the semicarbazone L1 was determined (Figure 1, also refer supporting information for details). The ligand crystallises as the E-isomer (Figure 1) with the N1-N2 and C1-C7 bonds in a trans disposition. The C8-O and C8-N2 (1.246(2) and 1.368(2) Å respectively) bonds are consistent with the keto (amide) tautomer.

The semicarbazone moiety is involved extensively in intermolecular H-bonding as shown in Figure 2. All three N-H protons donate H-bonds to either the semicarbazone O-atom (O1) or (intramolecularly) to the imine (N1). In fact all of the H-bonding interactions occur in this region of the molecule and the nitro group at the opposite end of the molecule in not involved at all in any way as an H-bond acceptor. The H-bonding pattern comprises a ribbon of L1 molecules each related by the 2-fold screw axis symmetry element in the direction of the *b* axis. Each ribbon is linked to a centrosymmetric ribbon via an H-bond donated by N2-H to O1 on a molecule above or below the plane of view in Figure 2 (not shown here for clarity).

The X-ray single crystal structure of the pyridyl-substituted semicarbazone L4.H_2O is shown in Figure 3. The ligand occupies a general site while a water molecule (not shown in Figure 3) is found

on a 2-fold axis (at half occupancy). Again the E-isomer of the Schiff base is present. The C8-O1 and C8-N2 bond lengths are consistent with the keto tautomer (1.244(2) and 1.366(2) Å respectively) and the N2-H proton was clearly seen in the difference electron density map.

H-bonding in this structure is distinctly different from that seen in L1. The syn oriented N2 (H)-C8-O1 moiety forms a centrosymmetric H-bonded dimer. Each dimer is linked to four others via H-bonds involving the terminal $–NH_2$ group (N3) and the carbonyl O-atom (O1) (Figure 4). The water bridges adjacent molecules through H-bonds made with pyridyl rings on either side.

Reaction of L1 with $Cu(OAc)_2$ led to the compound with the formula $[Cu_2(OAc)_2(L1)_2].(L1)_2$ Figure 5 shows the structure of the complex $[Cu_2(OAc)_2(L1)_2]$ which is a centrosymmetric dinuclear tetra-μ_2-(κO:κO′) acetato-bridged dicopper complex of ligand L1. Two of the L1 molecules are ligated by their semicarbazide O-atom to the axial coordination site of each Cu ion while the other 2 are not coordinated. All four L1 molecules are found in the keto tautomeric form and their internal bond lengths are not significantly different. In other words coordination of the O-donor has no bearing on the intramolecular bond lengths. Each Cu ion is coordinated by five O-donor ligands; four acetato ligands occupying the equatorial plane in addition to an axially bound semicarbazone. A strong Cu…Cu interaction is found (2.6378(7) Å). An intramolecular H-bond donated by the terminal $–NH_2$ group to an adjacent acetate ligand is apparent in Figure 5 and buttresses the Cu-O1a coordinate bond. The non-coordinated L1 molecule (not shown for clarity) forms several H-bonds within the structure, the most significant as an H-bond donor to one of the coordinated acetato O-donors (N2b-H…O4 2.30 Å).

Crystal structures of similar so-called ‘magic lantern’ tetraacetato-bridged dicopper(II) complexes abound in the literature [55-61] and more than 280 examples are to be found in the Cambridge Structural Database. Monodentate coordination through O1a would not normally be expected over bidentate (O1a/N2a) coordination accompanied by deprotonation at N3a. Perhaps the structural rigidity of the $Cu_2(OAc)_4$ core precludes coordination by anything except a monodentate ligand. Normally the reaction of such a ligand with Cu(II) in a ration 2:1 ratio ligand:copper would lead to a bis-chelate CuN_2O_2 complex with this reaction being assisted by deprotonation at N3a by a base such

as Et_3N, NaOH or NaOMe although base is not always required [62-65]. In this reaction the acetate anions could potentially accept a proton from N3a but instead they are consumed stoichiometrically in forming the $Cu_2(OAc)_4$ cluster. Formation of the Cu-acetate bonded complex using the semicarbazone ligands is consistent with reports in the literature [55-61] and reflect the inherent stability of the ($Cu_2(OAc)_4$) core.

Certain copper complexes of thiosemicarbazone and semicarbazone compounds are described to dissociate in solution [66]. For example for tridentate thiosemicarbazone, in frozen DMSO, the dimer remains intact, but in aqueous solution it converts to $[Cu(Fotsc)(H2O)]^+$ (Fotsc: formyl pyridine thiosemicarbazone).

The complexation reaction between Cu $(OAc)_2$ and L4 led to two distinct types of complexes with the same stoichiometry of metals and ligands. The first is shown in Figure 6 comprises a centrosymmetric monomeric compound bearing a pair of trans pyridyl-coordinated L4 ligands in addition to a pair of asymmetrically bound acetato ligands (Figure 6).

The Cu-O distances (Cu-O2 1.937(1) and Cu-O3 2.731(1) Å) are vastly different, the longer contact being too distant to be considered a proper coordinate bond. Thus the coordination geometry is basically distorted square planar. There is an extensive network of H-bonds that involve the non-coordinated water molecule and this is apparent in Figure 7.

It is noteworthy that none of the other atoms of the semicarbazone moiety was involved in the coordination of copper, including the O-donor of the semicarbazone group. This is contrary to the structure observed for the 4-nitrophenyl semicarbazone ligand wherein the C=O group of the semicarbazone was indeed involved in the coordination sphere of the copper. The superior pyridine donor is bound instead and again the ligand is not deprotonated thus disfavouring formation of an *N,O* chelate.

We also isolated a diuclear Cu complex from this reaction (Figure 8). Apart from the number of water molecules in the asymmetric unit, the Cu:ligand stoichiometry is the same as in the structure of monomeric $[Cu(OAc)_2(L4)_2].2H_2O$. The dimer occupies a crystallographic two-fold axis and one pair of symmetry related acetato ligands bridge the two metals in a $\mu_2\kappa$:O mode (through O3) while

another pair of acetates bind as monodentate terminal ligands (through O5). Again the pyridyl donor binds in preference to the semicarbazone moiety. The Cu…Cu distance is 3.476 Å in this particular bridging mode, which is also well known in the literature (more than 70 examples in the Cambridge Structural Database).

It is interesting that two complexes of the same metal:ligand stoichiometry have been isolated here. This can be rationalised by comparing the two Cu $(OAc)_2(L4)_2$ fragments as seen in Figure H viewed along the N-Cu-N axis. The monomeric complex finds the two trans acetato ligands oriented in an *anti* conformation such that the two weakly coordinated (or non-coordinated) O-atoms (O3) block the axial sites on both sides of the CuN_2O_2 plane thus preventing dimer formation. On the other hand in the structure of the dimer the acetato ligands are in a *syn* conformation (O4 and O6 are on the same side of the CuN_2O_2 plane). Now that O4 is out of the way, O3 is then able to act as a bridging ligand to another Cu ion and the dimer in Figure 9 (right) assembles.

The coordination modes of the copper complexes based on the X-ray crystallography as illustrated below (chart 2) for clarity and simplicity. As can be seen, depending on the ligands nature the coordination of the copper is altered although in most of the complexes acetate is involved and the copper is coordinated through the oxygen. In the case of ligand L1, the C=O of the semicarbazone moiety is also involved in the coordination as discussed previously. In the case of L1 the copper complex shows as a pentacoordinated species and L4 complex shows both a tetra and penta coordinated geometry. Thus the nature of the ligand seems to play a significant role towards the coordination modes of copper complexes. (see chart 2 below)

EPR spectral studies

EPR characteristics of copper complexes of several semicarbazones have not been described extensively in the literature although isopropyl group substituted thiosemicarbazones and semicarbazones have been described in the literature [67]. We have also examined the EPR spectra of the 4-nitrophenyl and 2-nitrophenyl copper acetate complexes. Two of the thiosemicarbazone EPR characteristics are also presented for comparative purposes.

Figure 10 shows the EPR spectrum of the 2-pyridyl semicarbazone (L6) copper complex in dimethyl sulfoxide at 140K. The upper panel shows the experimentally observed spectrum and the lower panel shows the simulated spectrum. It is evident from the spectra that there are four distinct lines observed in the spectra which is typical of a copper species. Figure 11 shows the EPR spectrum of the corresponding thiosemicarbazone (L5) copper complex under similar conditions The peaks are not well resolved in this case, however on subtraction of Savitzky-Golay (third order, 55 points) filtered data, the nitrogen super hyperfine spectra are revealed as predicted by the simulation. Figure 12 shows the 2-nitrophenylthiosemicarbazone (L7) copper complex monomer and Figure 13 shows the 4-nitrophenyl semicarabzone (L1) copper complexes respectively. The monomer of the 2-nitrophenyl semicarbazone (L8) copper complex is well resolved and the computer-simulated spectra coincide well. The EPR spectra of 4-nitrophenyl semicarbazone (L1) copper complex showed the presence of a momomer and a dimer. Panel **a** shows the experimental spectrum of both the species while panel **b** shows the computer simulated spectra for the above mixture. Panel **c** and **d** shows the simulated spectra for both the dimer and the monomer copper species. It is evident from the Figures that the experimental spectra are very close to simulated spectra. Further confirmation of the monomer and dimer species is provided by single crystal X-ray crystallographic studies for (see discussion in the X-ray section).

Table 1 shows the gx, gy and gz values observed for the respective copper complexes. For the 2-pyridyl semicarbazone (L6) the values ranged from 2.065-2.260. On the other hand the corresponding thiosemicarbazone (L5) showed values ranging from 2.050-2.185. The most striking features of the EPR spectral data were observed in the case of the monomer and dimer Cu-complexes of the nitrophenyl semicarbazone derivatives. The dimer showed a considerable increase in the gz value (2.300). In general the trend was similar for each of the complexes studied in the present study. Previous studies on 2-pyridine copper complexes showed values in the range of 2.114-2.029 at room temperature. [68-73] In another study by Raphael et al. [74] the N-4-substituted thiosemicarbazones showed a dimer consisting of two square pyramidal Cu(II) centers based on the EPR data and X-ray crystallography. Several other studies on this 2-pyridyl-methylsubstituted thiosemicarbazone yielded

a value ranging from 2.201-2.081[75-78]. The lower value observed in this complex can be attributed to the introduction of a methyl group in the structure of the 2-pyridine thiosemicarbazone. Based on the literature precedence on the characteristics of the EPR spectral interpretation we were able to ascertain that the following trend is associated with the copper complexes as described in the following paragraphs.

The complexes dissolved in DMSO showed typical EPR spectra of Cu^{2+} with four peaks at low field and one or two at high field. The EPR parameters determined from the spectra $g_{//} > g_{\perp}$ indicates that unpaired electron is predominantly in the dx2-y2 orbital and the copper ion has octahedral coordination. One of the compounds (2-pyridyl thiosemicarbazone) showed resolved nitrogen super hyperfine lines. The super hyperfine splittings were best fitted with three nitrogens coordinating to the copper. One of the compunds (2-nitrophenylsemicarbazone) showed peaks at zero field and at approximately 470 mT in addition to the peaks at g~2. These peaks could be simulated with a strongly exchange coupled Cu-Cu pair with anistropic dipole-dipole exchange interaction and a distance of approximately 2.74Å. These peaks could be simulated with a strongly exchange coupled Cu-Cu .Thus the EPR spectral data were consistent with the results obtained from X-ray single crystal studies for the copper complexes studied.

Biological studies:

Knowledge of the biological activity of novel chelators is key in determining their utility in future applications. To this end, the human prostate cancer PC-3 cell line was incubated with varied concentrations or doses (10, 50 and 100 μM) of the synthesized compounds to assess their biological activity. Caution should be exercised in terms of the solubility constraints of these thiosemicarbazones. The semicarbazones and the thiosemicarbazones were soluble in DMSO solvent (upto 10mg/ml) and therefore we chose this solvent to dissolve respective semicarbazones and thiosemicarbazones as well as the copper complexes used in the present study. As stated in the methods section, test compounds were solubilized in DMSO and then diluted into cell culture media to achieve desired final concentrations. Media were then sterile filtered before being added to wells containing PC3 cells. Final DMSO concentrations in media were <1.5% (v/v) and cellular

proliferation was compared to control wells containing equivalent concentrations of DMSO with no test compound. All test compound solutions that included copper were prepared using similar methods to achieve equivalent concentrations of test compound and copper. Thus if copper alone were causing cytotoxicity it would be expected to do so for all samples tested, which was not observed demonstrating that copper is not causing the toxicity to the cells. Table 2 shows determined IC_{50} values of all tested compounds.

The anticancer activity of several thiosemicarbazones have been previously examined and showed extremely high anti-proliferative activity, typically falling between 4.7-30 μM for the colon, lymphoma, cervical carcinoma, and neuroepithelioma cancer cell lines [26]. However, our interest was to find out the anti-proliferative effect in prostate cancer cell lines.

In the absence of copper, only 2-pyridyl thiosemicarbazone decreased cellular proliferation in our studies (Figure 14, Table 2) to a measurable extent; cells incubated with a range of concentrations of this ligand showed less than 50% cell proliferation compared to the untreated control cells. The other compounds in the series were found to be less potent or inactive under our experimental conditions for the cell lines investigated in this study. In comparison, copper-complexed derivatives showed a much larger influence on cellular proliferation (Figure15, Table 2). The copper-coordinated complexes showed varied efficacy in decreasing cellular proliferation following the trend 2-pyridyl thiosemicarbazone (L5) > 4-nitrophenyl thiosemicarbazone(L2) > 4-pyridyl thiosemicarbazone(L3) > 4-nitrophenyl semicarbazone(L1) > 4-pyridylsemicarbazone (L4)>2-pyridyl semicarbazone (L6). At all concentrations tested, cells incubated with L5+Cu showed no measureable cellular activity. This was also seen for cells incubated with 100 μM L2+Cu and L3+Cu. Lower concentrations of L2+Cu and L3+Cu showed higher levels of cellular proliferation; cells incubated with 10 and 50 μM L2+Cu showed proliferation at approximately 29 and 31% the rate of control cells respectively, while those incubated with 10 and 50 μM L3+Cu showed proliferation at approximately 29 and 31% the rate of control cells respectively, while those incubated with 10 and 50 μM L3+Cu showed proliferation at approximately 68 and 37% of controls respectively At all concentrations tested, cells incubated with L1+Cu, L4+Cu and L6+Cu showed proliferation rates similar to untreated controls. The above results

demonstrate that copper complexes of ligands L1, L4 and L6 are likely not useful as anticancer agents for the prostate. In contrast, copper complexes of L2 and L5 showed significant activity and from the structural consideration both these ligands contained a sulphur atom rather than oxygen (thiosemicarbazone vs semicarbazones). Therefore, we conclude that semicarbazones are generally non-active compared to thiosemicarbazones. This is consistent with literature reports [26] in which the introduction of a sulphur atom markedly improves the activity of these copper complexes of semicarbazones. Thus the observed results for copper chelates of a few thiosemicarbazones are interesting because of the marked biological activity displayed. It may be useful to explore these compounds further for therapeutic application for prostate cancer.

An interesting question arises as to why the copper complexes of ligand 2 and 3 differs in their biological activity? To address this issue we examine their X-ray crystal structures to examine the whether the coordination mode of the complex affects the biological profile. Examination of the crystal structure of the copper complexes revealed the following trend. The X-ray crystal structure of two of the complexes, the p-nitro substituted semicarbazone and the 4-pyridyl substituted semicarbazone indicated that the coordination of the copper was considerably altered For example, the nitro compound forms a copper –oxygen bond in the complex while the corresponding pyridyl compound does not form a bond between oxygen and it prefers the nitrogen center of the aromatic ring. In the first case, the copper is five coordinated (including the acetate ions) while in the second case it is a four coordinated species.

We do not have the crystal structure details for the L2 and L3 copper complexes, which possess similar structural features except that the oxygen is replaced with the sulphur (thiosemicarbazones) but on our intuition is that a similar behaviour for copper coordination is seen in these compounds. As can be seen from the biological data, the L3 copper complex shows a slight increase in activity compared to the L2 copper complex. Therefore a four coordinated pyridine copper complex seems to be slightly better than a nitro substituted compound. This is in accordance with the results obtained for a variety of copper complexes coordinated through the pyridine nitrogen atom [79]. In addition, studies have shown that coordination modes of copper complexes of Schiff bases derived from

coumarin based ligands does affect biological activity.[80] However, we stress that in solution state, the involvement of solvent molecules may disrupt the coordination of the copper ion which may be entirely different to that observed in the solid state.

PC-3 cells are an extensively studied disease model and in this case are used as an archetypal example of human cancer cell lines. Future studies will be required to determine variability in biological activities across alternate cell lines. Suffice to say that among the compounds examined in the present study, only the thiosemicarbazones possessed anticancer activity and none of the semicarbazones or their copper complexes exhibited significant biological activity. The activity shown by only thiosemicarbazones instead of any semicarbazones may be rationalized by potential structural differences. The canonical form of thiosemicarbazones compared to the semicarbazones is shown in Scheme 6. The tendency of sulphur compounds to form such an equilibrium is known and also the X-ray crystal structure of free ligands generally shows a C=O for semicarbazones while it tends to show the C-S bond somewhere between what is expected for a single and double bond. The superior activity shown by thiosemicarbazones is perhaps due to the reaction taking place in the cellular machinery shown in Scheme 7.

The above proposal is consistent to previous literature reports [81-84] relating to anti-HIV activity and anti-cancer activity of thiourea derivatives compared to urea derivatives. There is similarity between the structural features of thiourea compounds and thiosemicarbazones. In the above pathway there are three different mechanism which can affect cellular biochemical pathways. In the first pathway, a nucleophilic substitution by the OH is invoked. The hydroxyl anion from water or basic components in the cells attacks the double bond and releases the positive charge on the nitrogen atom to form the intermediate hydroxy thiol which subsequently eliminates the SH group and a proton to form the semicarbazone. In the second pathway, a free radical process is invoked in which hydroxyl free radical with a singlet oxygen radical species directly converts the thiosemicarbazone to the semicarbazone derivative by eliminating hydrogen sulfide and regenerating the hydroxyl radical once again. In the last pathway, the singlet oxygen generated by superoxide dismutases which acts as a radical quencher can combine with the sulphur atom of the thiosemicarbazone to give a sulfoxide or

sulfinic acid intermediate together with the formation of sulphur, sulphur dioxide and ammonium sulfate. It has been reported that, experimentally, chemical oxidation of thiourea derivatives with a N-bromosuccinamide and dioxane/water mixture forms the urea derivative [81]. In a similar manner sulphur containing thiosemicarbazones may affect the biochemical processes to exert its anti-cancer effects. Recently, a complete review of the anticancer activities of thiosemicarbazones has been reported [30]and the key biological role is often related with their capability to inhibit the enzyme ribonucleotide reductase, similar to what is observed with potent anticancer drugs such as triapine and methisazone.

Additional studies have also revealed that thiosemicarbazones can inhibit topoisomerase II enzyme. Serda et al [26] have conducted extensive studies with thiosemicarbazones and their studies of structure-activity relationship showed the chelators that utilized "soft" donor atoms, such as nitrogen and sulfur, resulted in potent anti-cancer activity. Indeed, the *N,N,S* donor atom set was crucial for the formation of redox active iron complexes that were able to mediate the oxidation of ascorbate. This further highlights the important role of generation of reactive oxygen species in mediating potent anti-cancer activity. Although this mechanism may be feasible in the ligands containing a sulphur atom in their structure, it is not known whether it occurs with copper complexes of these ligands since the sulphur atom of the thiosemicarbazones or oxygen atom of the semicarbazones coordinates with the copper.

Conclusions: Detailed studies on the structural characteristics of several semicarbazones and thiosemicarbazones have been conducted. The EPR spectral data showed that the copper complexes exhibit a similar type of coordination geometry to that observed for several other copper complexes described in the literature. The 4-nitrophenyl semicarbazone copper acetate complex formed both a monomer and dimer and the solution EPR study confirmed this. Further confirmation came from the X-ray single crystal studies. Interestingly we were able to observe that copper is only coordinated to the acetate anion and there was no evidence of formation of a copper complex between two thiosemicarbazone or semicarbazone ligands which was originally expected. This was despite the use of 2 moles of the ligand for every mole of copper ion. Biological studies on several of the copper

complexes of these ligands provided evidence that only thiosemicarbazone ligands and their copper complexes had any significant anticancer activity against prostate cancer cells. A mechanism for the biological activity shown by the thiosemicarbazone compounds is proposed which involves three different pathways involving a nucleophilic attack, a free radical pathway and finally a singlet oxygen induced by superoxide dismutase in the cells

Acknowledgements

The research work is partially supported from an ARC Linkage grant (LP 130100703 for DCR) from Australian Research Council, Australia. We also thank our colleagues in Center of Advanced Imaging, University of Queensland for their help during the course of this investigations.

References:

[1] J. Bernstein, H.L. Yale, K. Losee, M. Holsing, J. Martins, W. Lott, Journal of the American Chemical Society, vol. 73, 1951, pp. 906-912.
[2] B. Gingras, R. Somorjai, C. Bayley, Canadian Journal of Chemistry, vol. 39, 1961, pp. 973-985.
[3] T.S. Lobana, R. Sharma, G. Bawa, S. Khanna, Coordination Chemistry Reviews, vol. 253, 2009, pp. 977-1055.
[4] D.S. Kalinowski, Y. Yu, P.C. Sharpe, M. Islam, Y.-T. Liao, D.B. Lovejoy, N. Kumar, P.V. Bernhardt, D.R. Richardson, Journal of medicinal chemistry, vol. 50, 2007, pp. 3716-3729.
[5] W.E. Antholine, J.M. Knight, D.H. Petering, Journal of medicinal chemistry, vol. 19, 1976, pp. 339-341.
[6] K. Jensen, Zeitschrift für anorganische und allgemeine Chemie, vol. 221, 1934, pp. 11-17.
[7] K. Jensen, Zeitschrift für anorganische und allgemeine Chemie, vol. 221, 1934, pp. 6-10.
[8] M.J. Campbell, Coordination Chemistry Reviews, vol. 15, 1975, pp. 279-319.
[9] T. Lobana, S. Sandhu, Coordination Chemistry Reviews, vol. 47, 1982, pp. 283-300.
[10] P.S. Donnelly, Dalton Transactions, vol. 40, 2011, pp. 999-1010.
[11] D.X. West, A.E. Liberta, S.B. Padhye, R.C. Chikate, P.B. Sonawane, A.S. Kumbhar, R.G. Yerande, Coordination Chemistry Reviews, vol. 123, 1993, pp. 49-71.
[12] S.R. Turk, C. Shipman, J.C. Drach, Journal of general virology, vol. 67, 1986, pp. 1625-1632.
[13] R.W. Brockman, J.R. Thomson, M.J. Bell, H.E. Skipper, Cancer research, vol. 16, 1956, pp. 167-170.
[14] R.W. Brockman, Cancer research, vol. 2, 1955, pp. 1625.
[15] P.V. Bernhardt, L.M. Caldwell, T.B. Chaston, P. Chin, D.R. Richardson, JBIC Journal of Biological Inorganic Chemistry, vol. 8, 2003, pp. 866-880.
[16] M. Whitnall, J. Howard, P. Ponka, D.R. Richardson, Proceedings of the National Academy of Sciences, vol. 103, 2006, pp. 14901-14906.
[17] D.R. Richardson, P.C. Sharpe, D.B. Lovejoy, D. Senaratne, D.S. Kalinowski, M. Islam, P.V. Bernhardt, Journal of medicinal chemistry, vol. 49, 2006, pp. 6510-6521.
[18] G. Darnell, D. Richardson, Blood, vol. 94, 1999, pp. 781-792.
[19] L. Feun, M. Modiano, K. Lee, J. Mao, A. Marini, N. Savaraj, P. Plezia, B. Almassian, E. Colacino, J. Fischer, Cancer chemotherapy and pharmacology, vol. 50, 2002, pp. 223-229.
[20] P.V. Bernhardt, J. Mattsson, D.R. Richardson, Inorganic chemistry, vol. 45, 2006, pp. 752-760.
[21] D. Richardson, Antimicrobial agents and chemotherapy, vol. 41, 1997, pp. 2061-2063.

[22] T.B. Chaston, D.B. Lovejoy, R.N. Watts, D.R. Richardson, Clinical Cancer Research, vol. 9, 2003, pp. 402-414.
[23] D.S. Kalinowski, D.R. Richardson, Pharmacological reviews, vol. 57, 2005, pp. 547-583.
[24] T.B. Chaston, R.N. Watts, J. Yuan, D.R. Richardson, Clinical cancer research, vol. 10, 2004, pp. 7365-7374.
[25] D.S. Kalinowski, P. Quach, D.R. Richardson, Future medicinal chemistry, vol. 1, 2009, pp. 1143-1151.
[26] M. Serda, D.S. Kalinowski, N. Rasko, E. Potůčková, A. Mrozek-Wilczkiewicz, R. Musiol, J.G. Małecki, M. Sajewicz, A. Ratuszna, A. Muchowicz, 2014.
[27] P.M. Krishna, B. Shankara, N.S. Reddy, International Journal of Inorganic Chemistry, vol. 2013, 2013.
[28] H.D. Patel, S.M. Divatia, E. De Clereq, Indian J Chem B, vol. 52, 2013, pp. 535-545.
[29] L.N. Suvarapu, A.R. Somala, J.R. Koduru, S.O. Baek, V.R. Ammireddy, Asian Journal of Chemistry, vol. 24, 2012, pp. 1889-1898.
[30] S. Singhal, S. Aurora, S. Agarwal, N. Singhal, World Journal of Pharmacy and Pharmaceutical Sciences, vol. 2, 2013, pp. 4661.
[31] S. Lim, K.A. Price, S.-F. Chong, B.M. Paterson, A. Caragounis, K.J. Barnham, P.J. Crouch, J.M. Peach, J.R. Dilworth, A.R. White, JBIC Journal of Biological Inorganic Chemistry, vol. 15, 2010, pp. 225-235.
[32] M.A. Green, D.L. Klippenstein, J.R. Tennison, J Nucl Med, vol. 29, 1988, pp. 1549-1557.
[33] M.A. Green, C.J. Mathias, L.R. Willis, R.K. Handa, J.L. Lacy, M.A. Miller, G.D. Hutchins, Nuclear medicine and biology, vol. 34, 2007, pp. 247-255.
[34] Y. Fujibayashi, H. Taniuchi, Y. Yonekura, H. Ohtani, The Journal of Nuclear Medicine, vol. 38, 1997, pp. 1155.
[35] M. Oh, T. Tanaka, M. Kobayashi, T. Furukawa, T. Mori, T. Kudo, S. Fujieda, Y. Fujibayashi, Nuclear medicine and biology, vol. 36, 2009, pp. 419-426.
[36] A.L. Vāvere, J.S. Lewis, Nuclear medicine and biology, vol. 35, 2008, pp. 273-279.
[37] J.L. Dearling, J.S. Lewis, G.E. Mullen, M.J. Welch, P.J. Blower, JBIC Journal of Biological Inorganic Chemistry, vol. 7, 2002, pp. 249-259.
[38] S.I. Pascu, P.A. Waghorn, T.D. Conry, B. Lin, H.M. Betts, J.R. Dilworth, R.B. Sim, G.C. Churchill, F.I. Aigbirhio, J.E. Warren, Dalton Transactions, 2008, pp. 2107-2110.
[39] S.I. Pascu, P.A. Waghorn, B.W. Kennedy, R.L. Arrowsmith, S.R. Bayly, J.R. Dilworth, M. Christlieb, R.M. Tyrrell, J. Zhong, R.M. Kowalczyk, Chemistry–An Asian Journal, vol. 5, 2010, pp. 506-519.
[40] S.I. Pascu, P.A. Waghorn, T.D. Conry, H.M. Betts, J.R. Dilworth, G.C. Churchill, T. Pokrovska, M. Christlieb, F.I. Aigbirhio, J.E. Warren, Dalton Transactions, 2007, pp. 4988-4997.
[41] W.J. McBride, C.A. D'Souza, R.M. Sharkey, H. Karacay, E.A. Rossi, C.-H. Chang, D.M. Goldenberg, Bioconjugate chemistry, vol. 21, 2010, pp. 1331-1340.
[42] W.J. McBride, R.M. Sharkey, H. Karacay, C.A. D'Souza, E.A. Rossi, P. Laverman, C.-H. Chang, O.C. Boerman, D.M. Goldenberg, Journal of nuclear medicine, vol. 50, 2009, pp. 991-998.
[43] W.J. McBride, C.A. D'Souza, H. Karacay, R.M. Sharkey, D.M. Goldenberg, Bioconjugate chemistry, vol. 23, 2012, pp. 538-547.
[44] W.J. McBride, D.M. Goldenberg, R.M. Sharkey, Journal of Nuclear Medicine, vol. 55, 2014, pp. 1043-1043.
[45] P. Laverman, W.J. McBride, R.M. Sharkey, A. Eek, L. Joosten, W.J. Oyen, D.M. Goldenberg, O.C. Boerman, Journal of nuclear medicine, vol. 51, 2010, pp. 454-461.
[46] C.A. D'Souza, W.J. McBride, R.M. Sharkey, L.J. Todaro, D.M. Goldenberg, Bioconjugate chemistry, vol. 22, 2011, pp. 1793-1803.
[47] S. Lütje, G. Franssen, R. Sharkey, P. Laverman, E. Rossi, D. Goldenberg, W. Oyen, O. Boerman, W. McBride, Bioconjugate chemistry, vol. 25, 2014, pp. 335-341.
[48] M. Glaser, P. Iveson, S. Hoppmann, B. Indrevoll, A. Wilson, J. Arukwe, A. Danikas, R. Bhalla, D. Hiscock, Journal of Nuclear Medicine, vol. 54, 2013, pp. 1981-1988.

[49] T. Venkatachalam, G.K. Pierens, D.C. Reutens, Magnetic Resonance in Chemistry, vol. 52, 2014, pp. 98-105.
[50] G.M. Sheldrick, Acta Cryst A, vol. 64, 2008, pp. 112.
[51] L.J. Farrugia, Journal of Applied Crystallography, vol. 32, 1999, pp. 837-838.
[52] L.J. Farrugia, J. Appl. Cryst., 2012.
[53] A. Spek, Acta Crystallographica Section A: Foundations of Crystallography, vol. 46, 1990, pp. c34-c34.
[54] I. Antonini, F. Claudi, P. Franchetti, M. Grifantini, S. Martelli, Journal of medicinal chemistry, vol. 20, 1977, pp. 447-449.
[55] P. Larpent, A. Jouaiti, N. Kyritsakas, M.W. Hosseini, Dalton Transactions, vol. 43, 2014, pp. 2000-2006.
[56] Z. Chen, L. Liu, Y. Wang, H. Zou, Z. Zhang, F. Liang, Dalton Transactions, vol. 43, 2014, pp. 8154-8157.
[57] G. Durá, M.C. Carrión, F.A. Jalón, B.R. Manzano, A.M. Rodríguez, European Journal of Inorganic Chemistry, vol. 2013, 2013, pp. 5943-5957.
[58] F. Pavelčík, F. Hanic, Journal of Crystal and Molecular Structure, vol. 8, 1978, pp. 59-65.
[59] F. Wang, X.-Y. Wu, R.-M. Yu, Z.-G. Zhao, C.-Z. Lu, Journal of Coordination Chemistry, vol. 62, 2009, pp. 3296-3305.
[60] R. Sahu, S.K. Padhi, H.S. Jena, V. Manivannan, Inorganica Chimica Acta, vol. 363, 2010, pp. 1448-1454.
[61] J.-P. Zhang, Y.-Y. Lin, X.-C. Huang, X.-M. Chen, Journal of the American Chemical Society, vol. 127, 2005, pp. 5495-5506.
[62] S. Chandra, P. Ballabh, S. Choudhary.
[63] S. Chandra, S. Raizada, R. Verma, Journal of Chemical and Pharmaceutical Research, vol. 4, 2012, pp. 1612-1618.
[64] J.K. Swearingen, D.X. West, Transition metal chemistry, vol. 25, 2000, pp. 241-246.
[65] P. Paul, R.J. Butcher, S. Bhattacharya, Inorganica Chimica Acta, vol. 425, 2015, pp. 67-75.
[66] D.X. West, C.S. Carlson, A.E. Liberta, J.P. Scovill, Transition Metal Chemistry, vol. 15, 1990, pp. 383-387.
[67] S. Chandra, L.K. Gupta, Spectrochimica Acta Part A: Molecular and Biomolecular Spectroscopy, vol. 61, 2005, pp. 269-275.
[68] J.J. Allen, A.R. Barron, Dalton Transactions, 2009, pp. 878-890.
[69] Ł. Balewski, F. Sączewski, P.J. Bednarski, M. Gdaniec, E. Borys, A. Makowska, Molecules, vol. 19, 2014, pp. 17026-17051.
[70] C. Richardson, P.J. Steel, D.M. D'alessandro, P.C. Junk, F.R. Keene, Journal of the Chemical Society, Dalton Transactions, 2002, pp. 2775-2785.
[71] J. Xiang, Y. Luo, C.H. Wang, Zeitschrift für anorganische und allgemeine Chemie, vol. 639, 2013, pp. 563-568.
[72] R.R. Gagne, R.P. Kreh, J.A. Dodge, R.E. Marsh, M. McCool, Inorganic Chemistry, vol. 21, 1982, pp. 254-261.
[73] J. García-Tojal, A. García-Orad, J.L. Serra, J.L. Pizarro, L. Lezama, M.I. Arriortua, T. Rojo, Journal of inorganic biochemistry, vol. 75, 1999, pp. 45-54.
[74] P. Rapheal, E. Manoj, M.P. Kurup, Polyhedron, vol. 26, 2007, pp. 818-828.
[75] E.W. Ainscough, A.M. Brodie, J.D. Ranford, J.M. Waters, Journal of the Chemical Society, Dalton Transactions, 1991, pp. 2125-2131.
[76] E.W. Ainscough, A.M. Brodie, J.D. Ranford, J.M. Waters, Journal of the Chemical Society, Dalton Transactions, 1991, pp. 1737-1742.
[77] E.W. Ainscough, A.M. Brodie, J.D. Ranford, J.M. Waters, K.S. Murray, Inorganica chimica acta, vol. 197, 1992, pp. 107-115.
[78] S. Laly, G. Parameswaran, Thermochimica acta, vol. 168, 1990, pp. 43-51.
[79] I. Iakovidis, I. Delimaris, S.M. Piperakis, Molecular biology international, vol. 2011, 2011.

[80] B.S. Creaven, E. Czeglédi, M. Devereux, É.A. Enyedy, A.F.-A. Kia, D. Karcz, A. Kellett, S. McClean, N.V. Nagy, A. Noble, Dalton Transactions, vol. 39, 2010, pp. 10854-10865.
[81] O.J. D'Cruz, T.K. Venkatachalam, C. Mao, S. Qazi, F.M. Uckun, Biology of reproduction, vol. 67, 2002, pp. 1959-1974.
[82] O.J. D'Cruz, T.K. Venkatachalam, F.M. Uckun, Biology of reproduction, vol. 63, 2000, pp. 196-205.
[83] T. Venkatachalam, C. Mao, F.M. Uckun, Bioorganic & medicinal chemistry, vol. 12, 2004, pp. 4275-4284.
[84] T. Venkatachalam, E.A. Sudbeck, C. Mao, F.M. Uckun, Bioorganic & medicinal chemistry letters, vol. 11, 2001, pp. 523-528.

Figure captions:

Figure 1: ORTEP view of L1(30% probability ellipsoids) showing the atomic nomenculture

Figure 2: PLATON view of H-bonding in the structure of compound L1

Figure 3: ORTEP plot (30% probability ellipsoids) of L4 (water molecule not shown)

Figure 4: PLATON view of the H-bonding in compound L4.H_2O

Figure 5: ORTEP plot(30% probability ellipsoids) of $[Cu_2(OAc)_4(L1)_2]$. Selected bond lengths (Å): Selected bond lengths (Å): Cu(1)-O(2) 1.956(2); Cu(1)-O(3) 1.957(2); Cu(1)-O(1) 1.971(2); Cu(1)-O(4) 1.973(2); Cu(1)-O(1A) 2.243(2); Cu(1)-Cu(1)′ 2.6378(7).

Figure 6. ORTEP plot (30% probability ellipsoids) of $[Cu(OAc)_2(L4)_2]$ (water molecule omitted). Selected bond lengths (Å): Cu(1)-N(1) 2.038(1); Cu(1)-O(2) 1.937(1); Cu(1)…O(3) 2.731(1).

Figure 7: PLATON view of the Figure G. PLATON view of the $[Cu(OAc)_2(L4)_2].2H_2O$ unit cell showing H-bonding interactions unit cell showing H-bonding interactions.

Figure 8: ORTEP view of dimeric $[Cu_2(OAc)_4(L4)_4].9H_2O$ (30% probability ellipsoids). Water moelcules omitted. Selected bond lengths (Å): Cu(1)-N(1) 2.007(3); Cu(1)-N(5) 2.022(3); Cu(1)-O(3) 1.972(3); Cu(1)-O(5) 1.924(3) Cu(1)-O(3′) 2.560(3).

Figure 9: Figure H. PLATON views of the monomeric (left) and dimeric (right) Cu complexes of L4 viewed along the N-Cu-N axis (H-atoms and water molecules omitted for clarity). The different orientation of the acetato ligands is apparent.

Figure 10. EPR spectrum of 2-pyridylsemicarbazonecopper. a) experimental b) computer simulation. Peaks corresponding to a second species not included in the simulation are marked with an asterisk.

Figure 11

EPR spectrum of 2-pyridylthioscarbazonecopper. a) experimental b) computer simulation, c) experimental spectrum after subtracting Savitzky-Golay (third order, 55 points) filtered data to reveal nitrogen superhyperfine, d) computer simulation of the filtered data.

Figure 12

EPR spectrum of 2-nitrophenylthiosemicarbazonecopper. a) experimental b) computer simulation. Peaks corresponding to a second species not included in the simulation are marked with an asterisk.

Figure 13

EPR spectrum of 4-nitrophenylsemicarbazonecopper (**C3&C2)** a a) experimental b) computer simulation. Peaks from the dimeric species are marked with an asterisk.

Figure 14 Ligands activity towards cancer cells in dimethylsulfoxide medium

Figure 15. Copper complexes of ligands activity towards cancer cells in dimethyl sulfoxide medium

Figures

Figure 1

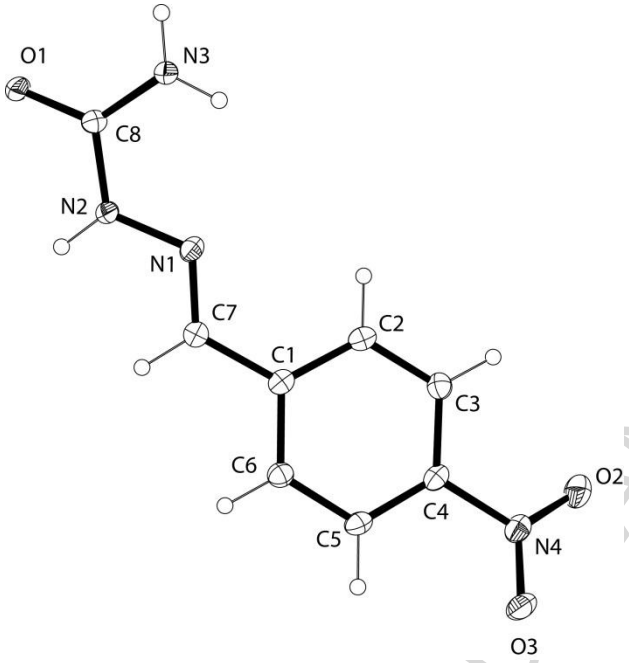

Figure 2:

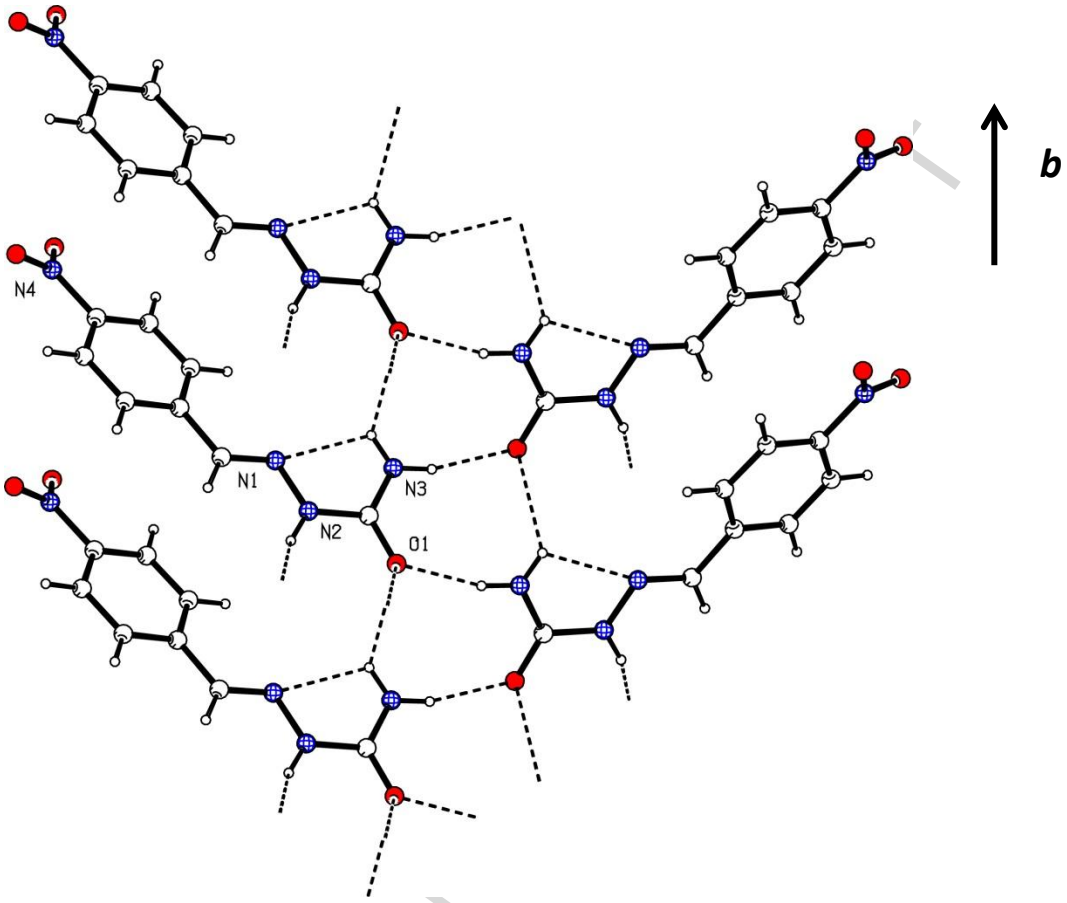

Figure 3

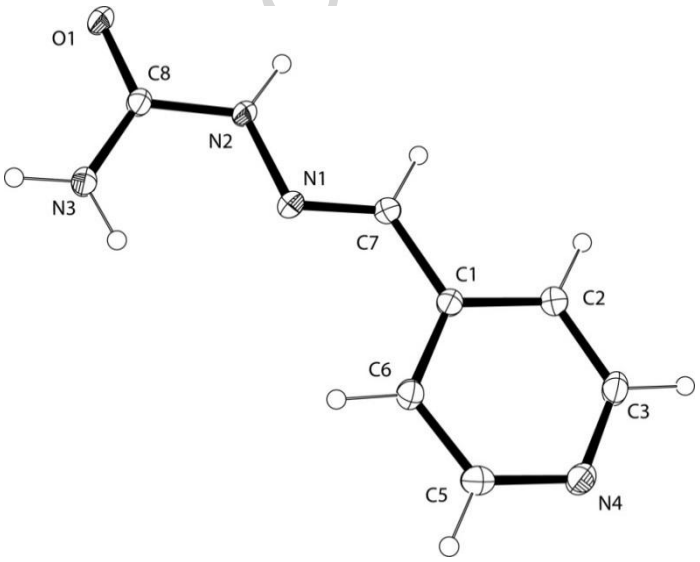

Figure 4

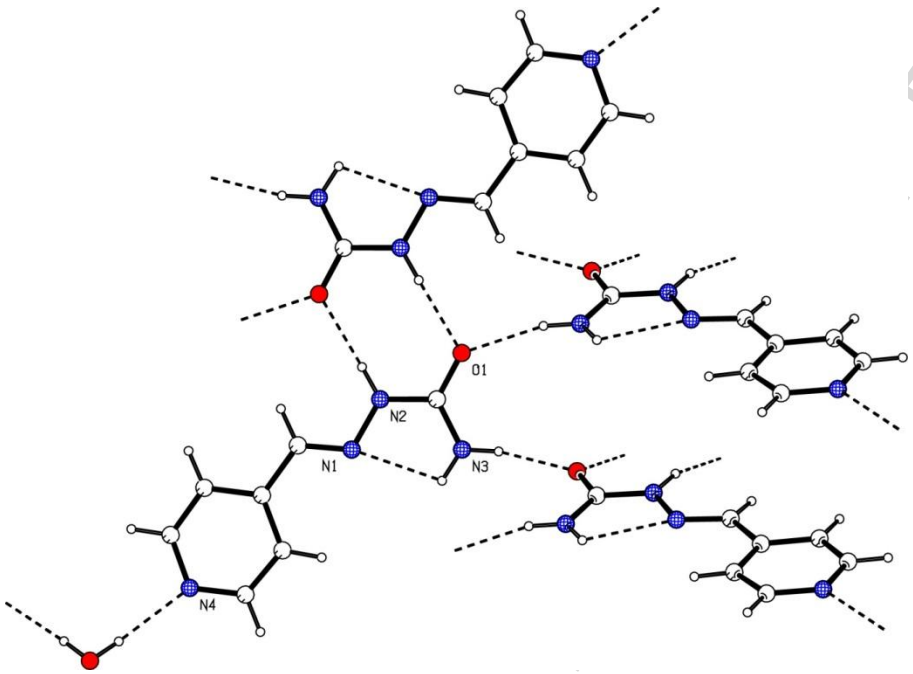

Figure 5

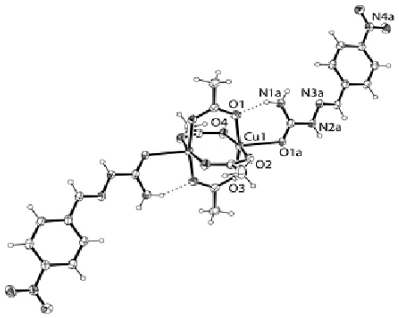

or

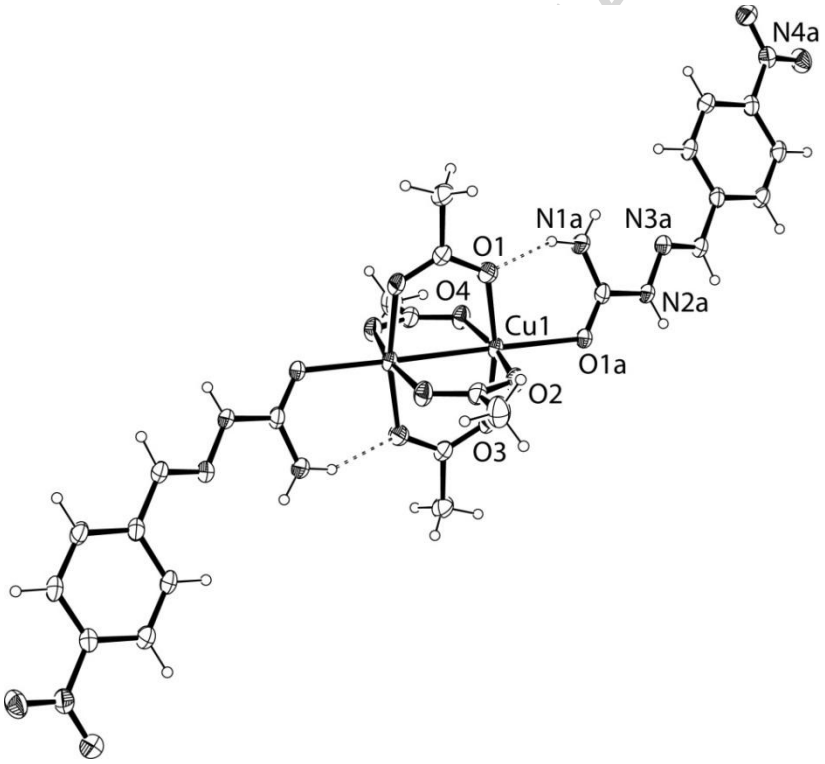

Figure 6

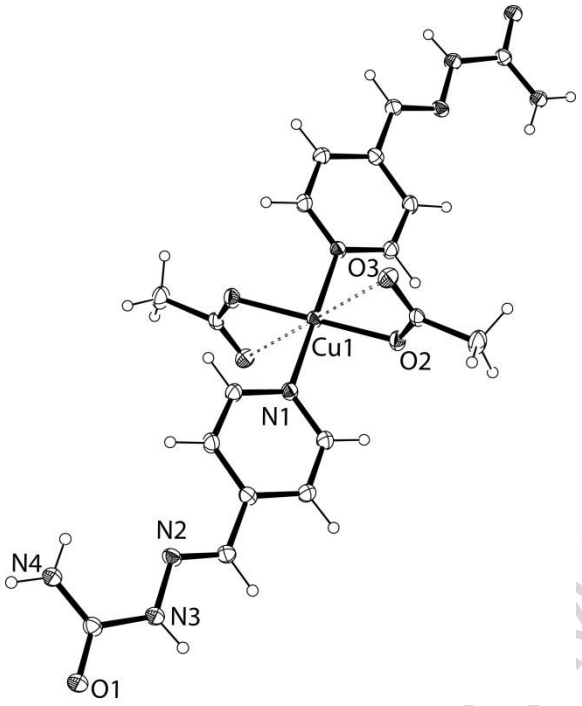

Figure 7

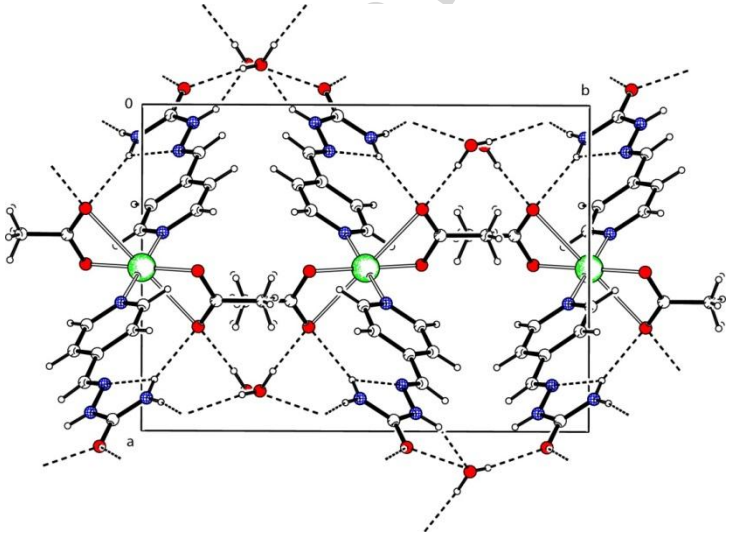

Figure 8

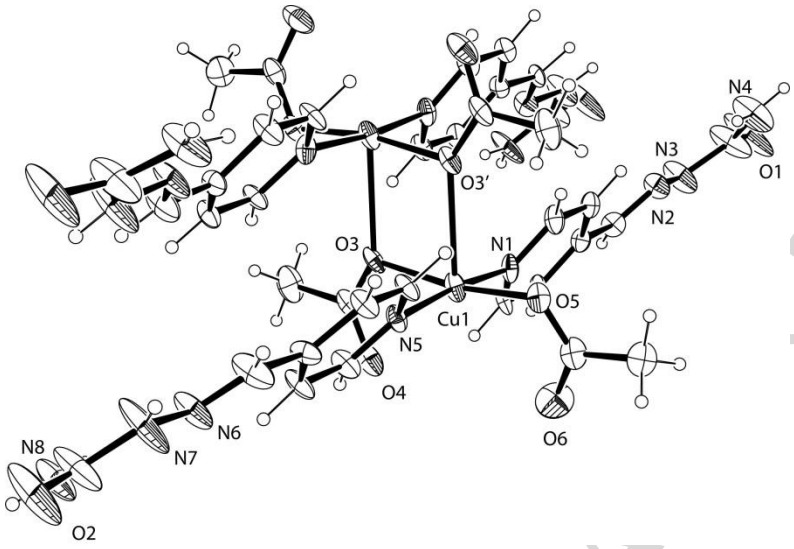

Figure 9

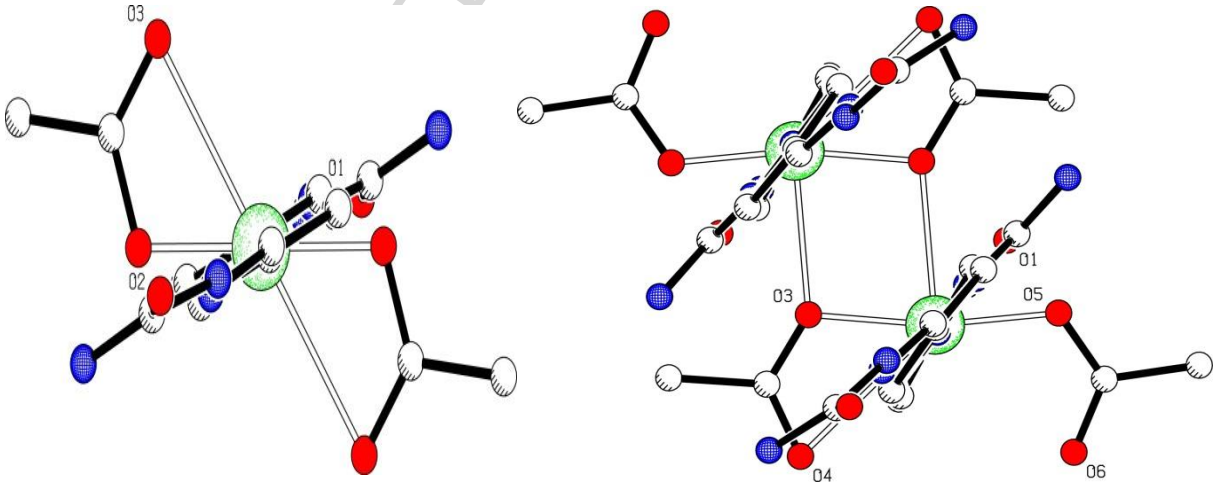

Figure 10

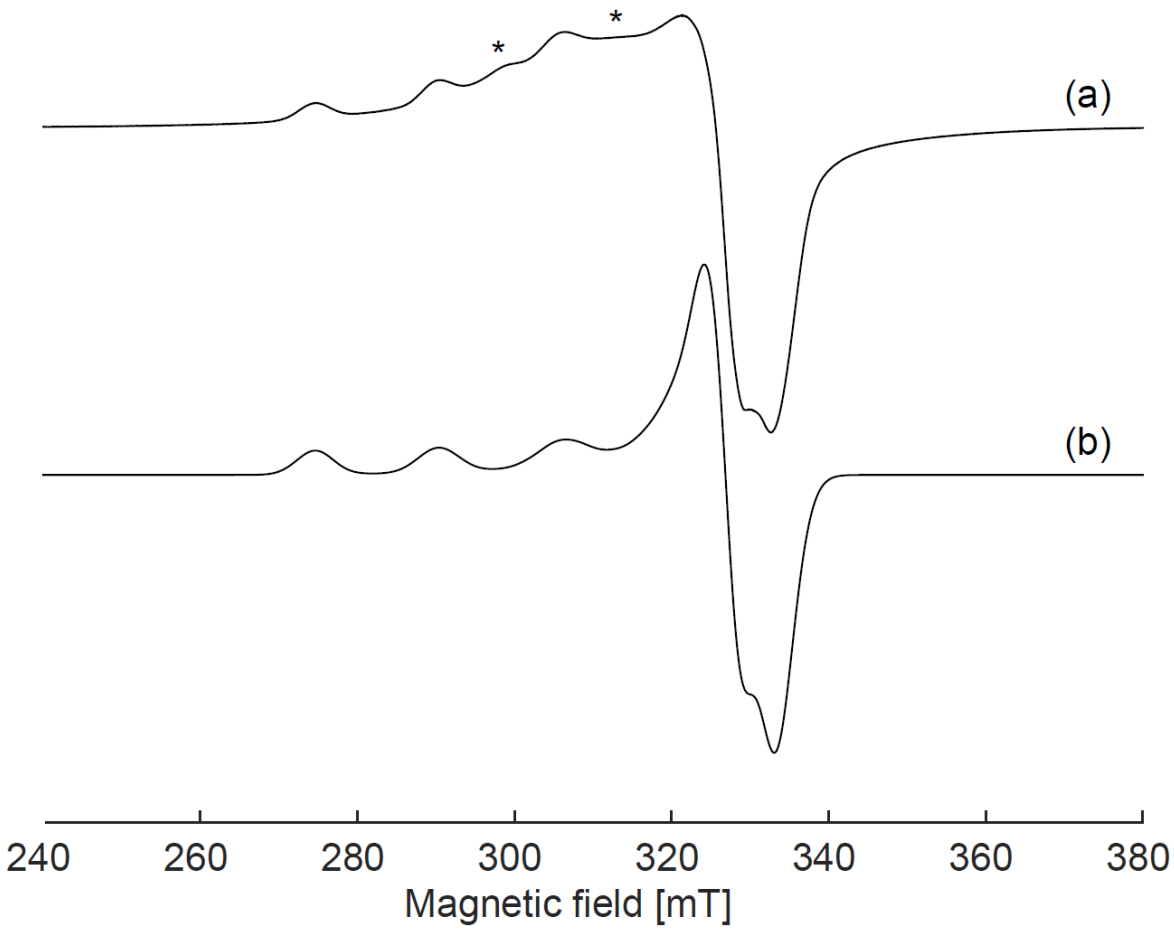

Figure 11

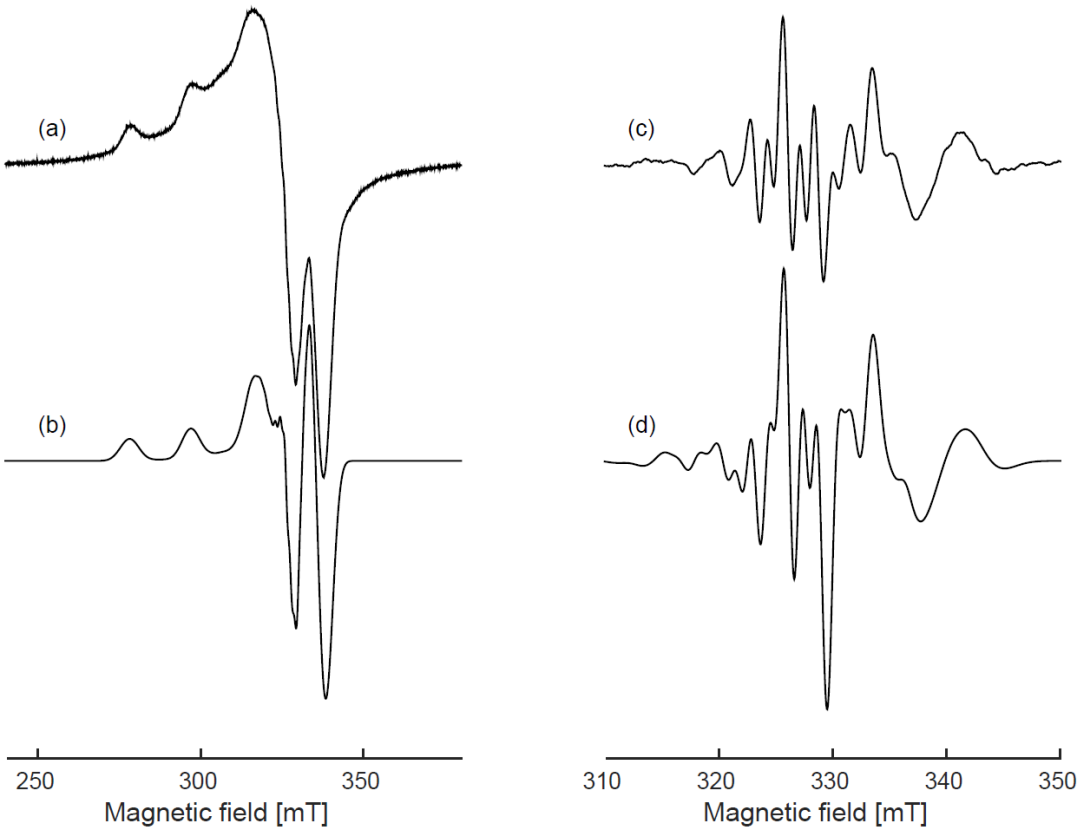

Figure 12

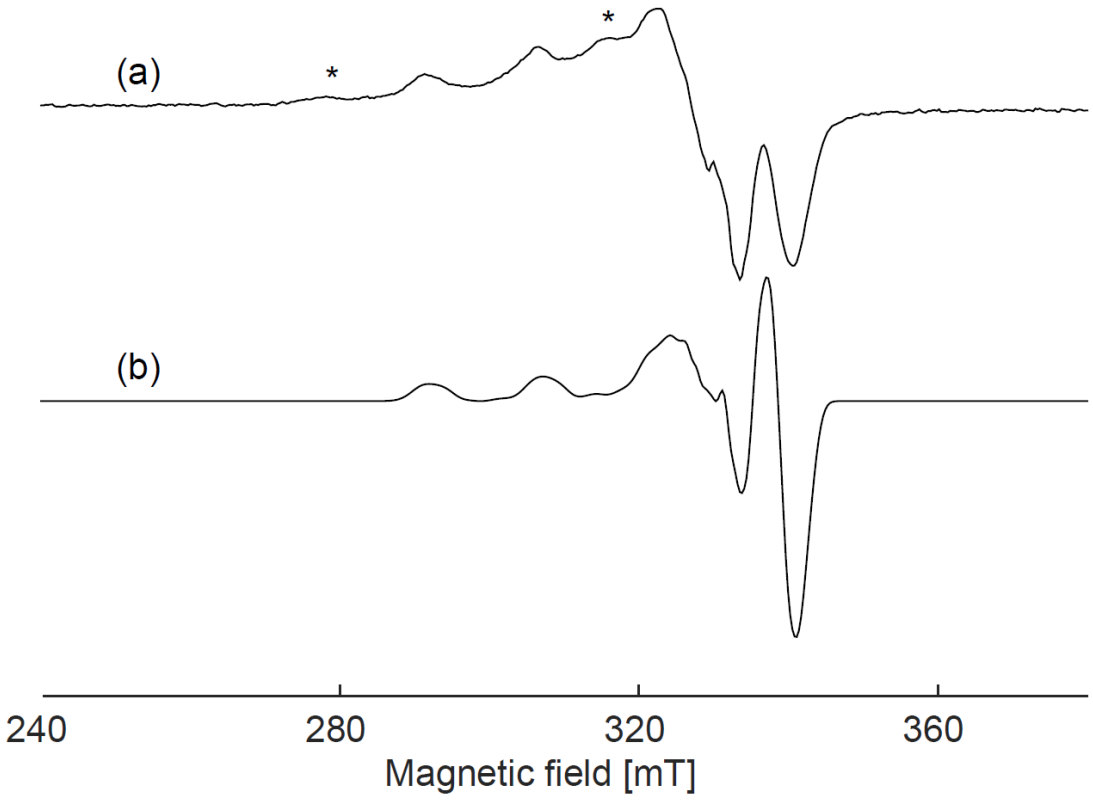

Figure 13

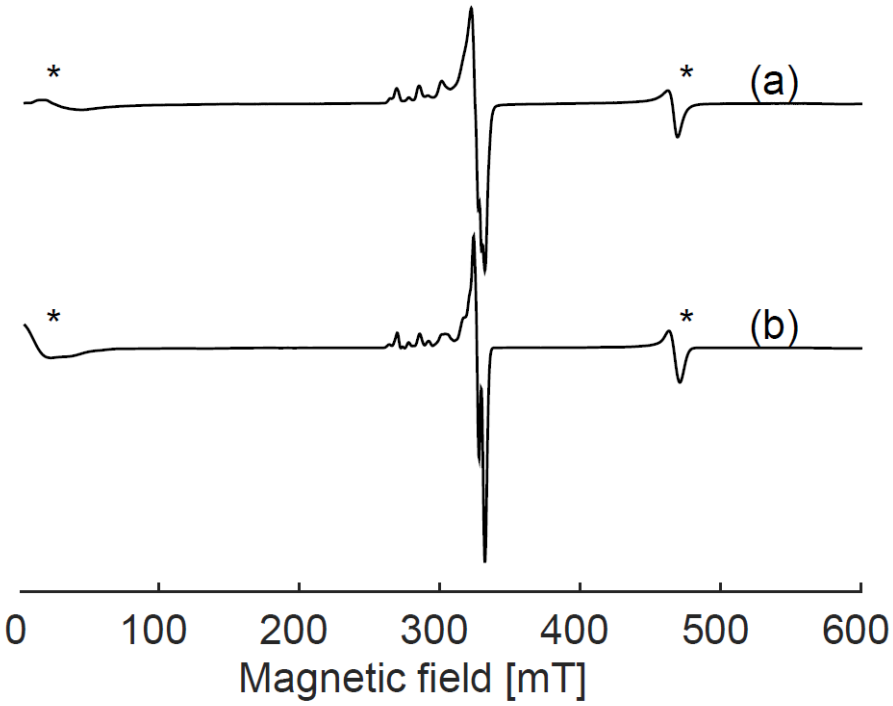

Figure 14

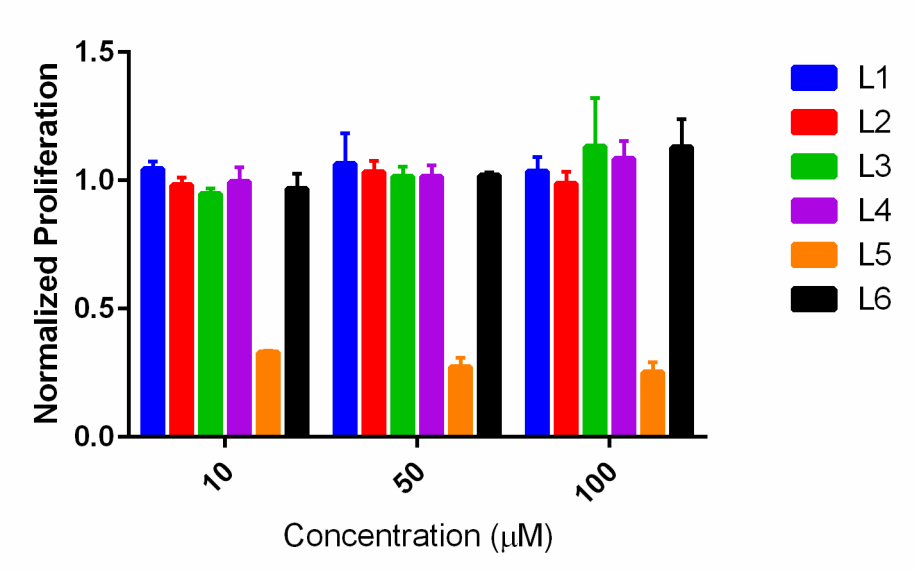

Figure 15

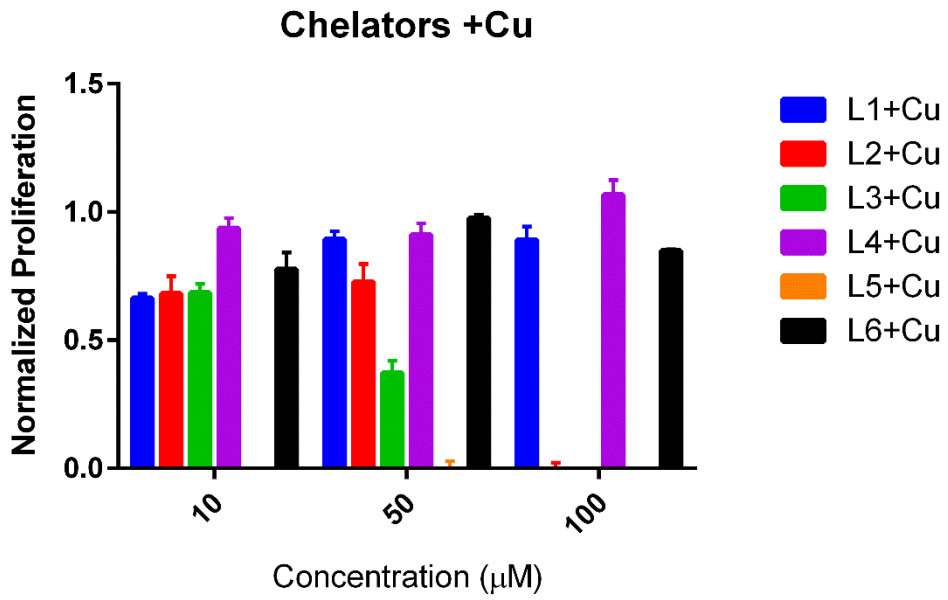

Tables:

Table 1: g values obtained for some of the copper complexes of semi and thiosemicarbazones

Table 2: IC_{50} values determined for each of the test compound

Table 1:

	2-pyridylsemicabazone (L6)	2-pyridylthiosemicarbazone (L5)	p-nitrophenylsemicarbazone dimer(C3)	p-nitrophenylsemicarbazone monomer (C2)	2-nitrophenylthiosemicarbazone (L8)
gx	2.055	2.050	2.040	2.060	2.025
gy	2.065	2.050	2.040	2.060	2.028
gz	2.260	2.185	2.300	2.290	2.140
Ax ($10^{-4}cm^{-1}$)	10.0	40.0	10.0	10.0	25.0
Ay ($10^{-4}cm^{-1}$)	10.0	10.0	10.0	10.0	25.0
Az ($10^{-4}cm^{-1}$)	162.0	188.0	164.0	170.0	152.0
Ax_N ($10^{-4}cm^{-1}$)		13.0			10
Ay_N ($10^{-4}cm^{-1}$)		13.0			10
Az_N ($10^{-4}cm^{-1}$)		14.0			11
D (cm^{-1})			0.131		
r (Å)			2.74		

Table 2

Ligand	Chelator Alone (µM)	Chelator + Cu (µM)
L1	>100	>100
L2	>100	<10
L3	>100	33
L4	>100	>100
L5	<10	<10
L6	>100	>100

Chart captions

Chart 1: Chart depicting the Keto-entol tautomerism of semicarbazones

Chart 2: Coordination modes of few of the copper complexes observed for semicarbazones

Chart 1:

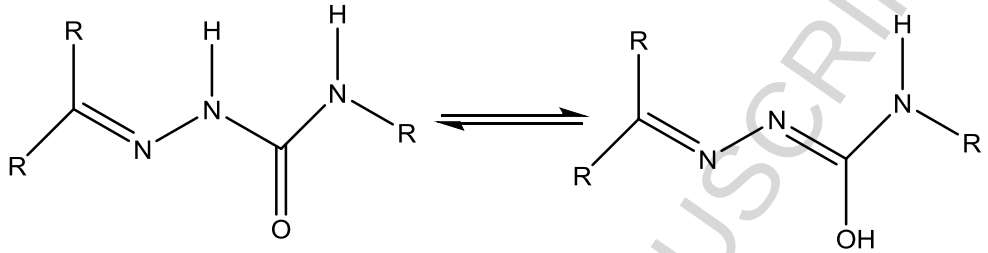

Keto enol

Chart 2

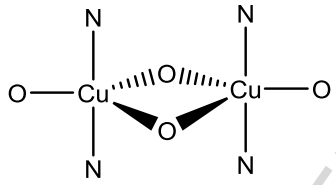

$[Cu_2(OAc)_4(L4)_4]9H_2O$

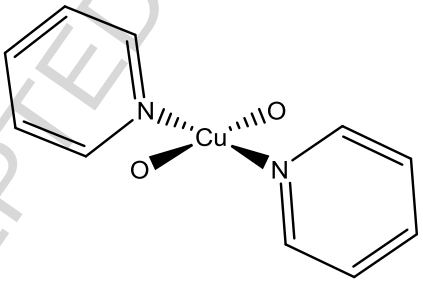

$[Cu(OAc)_2(L4)_2]$

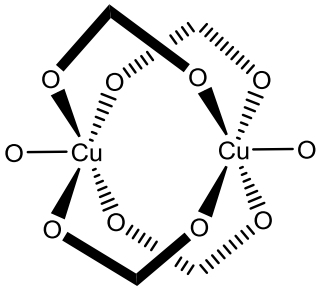

$[Cu_2(OAc)_4(L1)_2]$

Highlights

*Synthesis of semicarbazones and thiosemicarbazones

*Synthesis of Copper complexes of semicarbazones

*Single crystal X-ray studies of copper complexes

*EPR studies of copper complexes

*Biological activity of copper complexes of thiosemicarbazones and semicarbazones

Graphical Abstract

Synthesis, characterisation and biological activities of semicarbazones and their copper complexes.

Taracad.K.Venkatachalam*, Paul. V. Bernhardt[#], Chris.J.Noble, N.Fletcher, Gregory.K.Pierens, Kris.J.Thurecht, David.C.Reutens (Centre for Advanced Imaging, [#]School of Chemistry University of Queensland, St.Lucia, Brisbane 4072, Australia.

Abstract: Substituted semicarbazones have been prepared and their single crystal structure was determined. Electron paramagnetic resonance of few of the copper complexes showed consistent trend to those observed by single crystal X-ray crystallography. Interestingly, only the copper complexes of thiosemicarbazone showed anticancer activity.